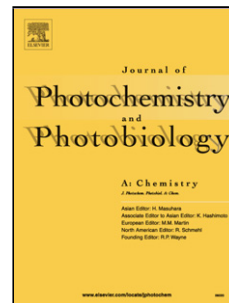


Accepted Manuscript

Title: A highly selective, pH-tolerable and fast-response fluorescent probe for Fe³⁺ based on star-shape benzothiazole derivative

Authors: Kai Jiang, Yan-Cheng Wu, Han-Qing Wu, Shu-Li Li, Shi-He Luo, Zhao-Yang Wang



PII: S1010-6030(17)31063-8
DOI: <https://doi.org/10.1016/j.jphotochem.2017.09.065>
Reference: JPC 10912

To appear in: *Journal of Photochemistry and Photobiology A: Chemistry*

Received date: 18-7-2017
Revised date: 9-9-2017
Accepted date: 25-9-2017

Please cite this article as: Kai Jiang, Yan-Cheng Wu, Han-Qing Wu, Shu-Li Li, Shi-He Luo, Zhao-Yang Wang, A highly selective, pH-tolerable and fast-response fluorescent probe for Fe³⁺ based on star-shape benzothiazole derivative, *Journal of Photochemistry and Photobiology A: Chemistry* <https://doi.org/10.1016/j.jphotochem.2017.09.065>

This is a PDF file of an unedited manuscript that has been accepted for publication. As a service to our customers we are providing this early version of the manuscript. The manuscript will undergo copyediting, typesetting, and review of the resulting proof before it is published in its final form. Please note that during the production process errors may be discovered which could affect the content, and all legal disclaimers that apply to the journal pertain.

A highly selective, pH-tolerable and fast-response fluorescent probe for Fe³⁺ based on star-shape benzothiazole derivative

Kai Jiang^a, Yan-Cheng Wu^{ab*}, Han-Qing Wu^a, Shu-Li Li^a, Shi-He Luo^a, and Zhao-Yang Wang^{*a}

^a School of Chemistry and Environment, South China Normal University; Key Laboratory of Theoretical Chemistry of Environment, Ministry of Education, Guangzhou 510006, China

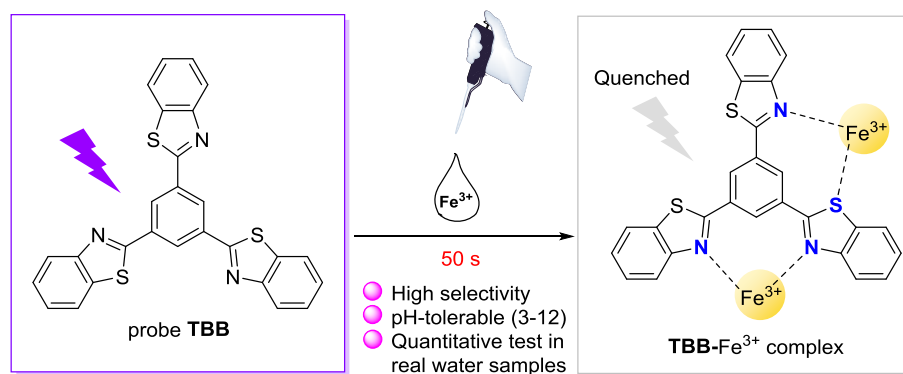
^b College of Materials Science and Engineering, South China University of Technology, Guangzhou 510640, China.

* Corresponding Author

E-mail: wangzy@scnu.edu.cn. Tel: 8620-39310258.

E-mail: wuycity@gmail.com.

Graphical abstract



Highlights

- The star-shape probe TBB is highly selective towards Fe³⁺ over other metal ions.
- TBB shows fast response (50 s) and good pH-tolerance (3-12) on detecting Fe³⁺.
- TBB is applied for the quantitative detection of Fe³⁺ in real water samples.
- The 1:2 binding mode for TBB-Fe³⁺ complex has been confirmed.
- The dynamic quenching mechanism has been proved by TCSPC experiments.

Abstract

A star-shape benzothiazole-based molecule **TBB**, obtained through a simple condensation reaction of 2-aminothiophenol with 1,3,5-benzenetricarboxylic acid in the presence of available catalyst polyphosphoric acid (PPA), has been exploited as a highly selective fluorescent Fe^{3+} probe over other metal ions in aqueous media ($\text{H}_2\text{O}/\text{THF}$, $v/v = 4/6$). For this fast-response probe with a response time of 50 s, its quenching mechanism involving in the combination of static and dynamic quenching is confirmed by the test of time-correlated single photon counting (TCSPC) experiments. Noticeably, the probe **TBB** is suitable for Fe^{3+} detection in a wide pH range (3-12) of aqueous solution, and it can be successfully applied for Fe^{3+} quantitative measurement in real water samples.

Keywords: Star-shape benzothiazole derivative; Fluorescent probe; Highly selective Fe^{3+} detection; pH-tolerable; Fast-response

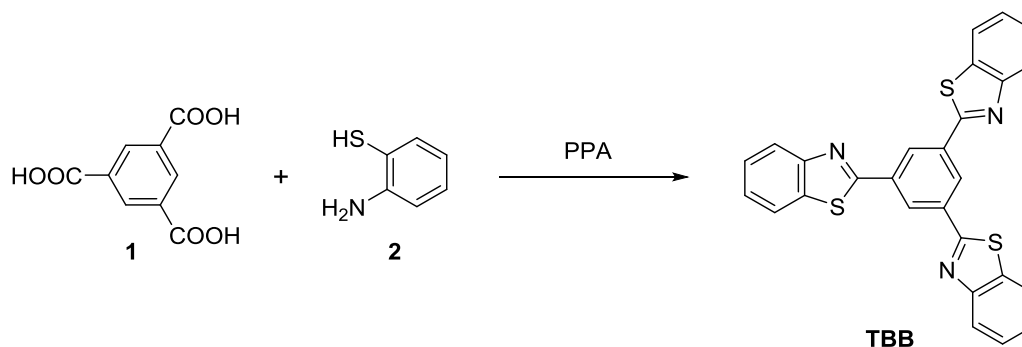
1. Introduction

As the most abundant transition metal in the human body, iron is closely related to some crucial physiological process, such as cellular metabolism, oxygen uptake and electron transfer, etc [1,2]. The deficiency of iron can induce the anaemia and neurodegenerative diseases, while overload of iron might oxidize and finally damage cellular components [3-5]. In addition, excessive iron in water brought about serious environmental problems. The U.S. Environmental Protection Agency (EPA) has set a limit of iron in drinking water and food to 0.3 ppm ($\sim 5.4 \mu\text{M}$) [6,7]. Therefore, the detection of trace iron ion in real water samples or under wide-range pH environment is highly desirable [3,8-18]. However, the reported Fe^{3+} probes partially exhibited some obvious drawbacks, such as synthetic difficulty [19,20], unsatisfactory selectivity [21-23], interference from pH [24,25] and time-consuming [26,27], which negatively affected their properties and application. Thus, it is meaningful to exploit more available, selective, time-saving and practical probe for detection of Fe^{3+} .

Usually, benzothiazole compounds are widely used in pharmaceutical field for their pharmacological activities [28,29]. In recent years, benzothiazole derivatives with extensively conjugate structures have been applied in the field of photoelectric materials [30-32]. At the same time, due to the existence of binding sites from N and S atoms [33,34], some benzothiazole-based fluorescent probes with high quantum yield and large Stokes shift have been designed also [35,36]. However, for the less reported benzothiazole-based Fe^{3+} probes [37], it is still necessary to improve selectivity [38], enhance pH tolerance [39], and reduce responding time [40]. In a word, for the detection of Fe^{3+} with high selectivity, broad pH-tolerability and fast response, the

development of benzothiazole-based fluorescent probe with better sensing performance is in encouragement.

Herein, a star-shape molecule tri-benzothiazolyl benzene (**TBB**) is synthesized through a simple reaction (**Scheme 1**), which can function as an excellent optical probe for Fe^{3+} with dual discriminating channels, i.e. detectable color change in room light and fluorescent ‘turn-off’ response. The probe **TBB** shows not only great selectivity, good sensitivity and rapid response towards Fe^{3+} , but also availability within a broad range of pH environment and real water samples. Meanwhile, the 1:2 binding mode between **TBB** and Fe^{3+} has been demonstrated by Job’s plots and ESI-MS spectrum. What’ more, Stern-Volmer plots and time-correlated single photon counting (TCSPC) experiments have been carried out to elucidate a static and dynamic hybrid quenching process.



Scheme 1. Synthetic route for **TBB**.

2. Experimental

2.1. Chemicals and apparatus

All chemicals used within this work were of analytical grade purity. The salts, such as KNO_3 , NaNO_3 , AgNO_3 , $\text{Cu}(\text{NO}_3)_2$, $\text{Fe}(\text{NO}_3)_3$, $\text{Zn}(\text{NO}_3)_2$, $\text{Ca}(\text{NO}_3)_2$, $\text{Mg}(\text{NO}_3)_2$, $\text{Al}(\text{NO}_3)_3$, HgCl_2 , $\text{Cd}(\text{NO}_3)_2$, CrCl_3 ,

FeSO₄, Co(NO₃)₂, BaCl₂, NiSO₄, Pb(NO₃)₂, were used as metal ions sources. ¹H NMR spectrum was collected on a BRUKER DRX-400 spectrometer in CDCl₃ using TMS as an internal standard. Positive ions mass spectra (ESI-MS) were recorded on a Thermo LCQ DECA XP MAX mass spectrometer. IR spectrum was performed on a BRUKER VECTOR33 and UV-*vis* absorption spectra were measured by using a Shimadzu UV-2700 ultraviolet absorption detector at room temperature. The fluorescence spectra were recorded with a Hitachi F-4600 spectrophotometer at room temperature. pH values were measured by a PHS-25C meter. Fluorescence lifetime was measured by FLS 920 Fluorescence Spectrometer.

2.2. Methods

2.2.1. General procedure for spectra measurements

The probe **TBB** was dissolved in THF to acquire 1 mM stock solution. The measurements of both UV-*vis* absorption and fluorescence spectra were conducted in 10 μM aqueous solution under room temperature. For fluorescence measurements, both the excitation and emission slit widths were set at 5 nm.

2.2.2. Limit of detection

The limit of detection (LOD) was determined by using equation: $LOD = 3\delta/K$. Herein, δ is the standard deviation of the blank measurements ($n = 10$), and the K is the slope of the calibration curve.

2.2.3. Calculation of Stern-Volmer constant

The Stern-Volmer quenching constant (K_{sv}) was calculated according to the Stern-Volmer equation: $I_0/I = K_{sv}[Q] + 1$, where I_0 and I are the fluorescence intensities observed in the absence and presence of Fe^{3+} , respectively. $[Q]$ is the quencher concentration.

2.3. Synthesis of probe **TBB**

Referring to the literature [41], 1,3,5-benzenetricarboxylic acid **1** (5 mmol), 2-aminothiophenol **2** (15.5 mmol) and 25 mL polyphosphoric acid (PPA) were added into a 50 mL round bottom flask. After stirring for 24 h under 150 °C, the reaction was stopped by adding water and then the mixture was regulated to the pH range of 9-10 with sodium hydroxide. The crude product was obtained by filtration, and the further purification by recrystallization with dichloromethane gave the target compound tri-benzothiazolyl benzene (**TBB**) as a white solid (481 mg, yield 33.6%), m.p. > 300 °C; 1H NMR (400 MHz, $CDCl_3$, TMS), δ : 7.43-7.50 (m, 3H), 7.53-7.60 (m, 3H), 7.99 (d, $J = 8.0$ Hz, 3H), 8.18 (d, $J = 8.0$ Hz, 3H), 8.93 (s, 3H); IR (film), ν , cm^{-1} : 3055, 1632, 1501, 1418, 1314, 1190, 766, 752, 719; ESI-MS, m/z (%): Calcd for $C_{27}H_{16}N_3S_3$ ($[M+H]^+$): 478.04 (100). Found: 478.25 (100) [their corresponding characterization spectra as **Figs. S1-S3** can be seen in Supporting Information (**SI**)].

3. Results and discussion

3.1. Absorption and fluorescence studies of probe **TBB** in solution

In order to choose the solvent for probe solution, solvatochromism behavior of probe **TBB** (10 μ M) was examined in nonpolar and polar solvents, such as PhMe, CH_2Cl_2 , THF, EtOAc, $CHCl_3$, DMF and EtOH. The photophysical data (see **Figs. S4-S5** and **Table S1** in **SI**) show that there are no significant changes among different tested solvents. Due to the good miscibility with water and

relatively high fluorescence intensity, THF was finally chosen as constituent of the aqueous solution.

It will be more valuable if probes can detect metal ion in aqueous solution. Therefore, the emission property in different H₂O/THF systems was initially investigated. As shown in **Fig. 1**, the main emission bands are located at nearly 380 nm and the fluorescence intensity exhibits no obvious change within the range of water fraction between 0% and 40%. With the increase of water fraction over 50%, there is a slight change. These results show that **TBB** has a certain tolerance to water. However, the fluorescence intensity of **TBB** in H₂O/THF solution dramatically decreases when the fraction of water achieves to 70%. This result is in accordance with the UV-vis absorption spectra of **TBB** in the different ratio of H₂O/THF solution (**Fig S6**). And as the water fraction is equal to or over 70%, there are obvious level-off tails in longer wavelength region, implying the fluorescence quenching caused by the aggregation of **TBB** in large amount of water [42]. Thus, the suitable solution system should be selected as a H₂O/THF of 4/6 (v/v).

3.2. Optical response towards Fe³⁺

From the UV-vis absorption spectra (**Fig. 2**), it is apparent that the prominent absorption bands peak at 231 nm, 254 nm and 313 nm, which can be aligned with n- π^* , π - π^* and n- π^* electronic transition. Thereinto, the band at 313 nm is ascribed to the benzothiazole group [43]. Particularly, the addition of Fe³⁺ causes linear growth of absorption peak at 313 nm along with visible color change (**Fig. S7**). This can be assigned to the formation of metal-**TBB** ground-state complexes [12,44,45], not resulting from the absorption of Fe³⁺ itself (**Fig. S8**).

To further investigate the efficiency of probe **TBB** toward Fe^{3+} , the fluorometric titration experiment has been carried out. As shown in **Fig. 3**, the fluorescence spectrum of **TBB** in THF- H_2O displays a major emission peak at 387 nm and a shoulder band at 374 nm. A gradual decrease of the fluorescence intensity of **TBB** at both peaks can be observed upon progressive addition of Fe^{3+} , and the quenching efficiency achieves to 95.3% when the amount of Fe^{3+} comes to 1 mM. The fluorescence intensity at 387 nm is proportional to the concentration of Fe^{3+} in the range of 0 - 0.5 mM (**Fig. S9**). Thus, the corresponding detection limit can be calculated to be 3.05×10^{-6} M (0.17 ppm) [10]. This value is lower than not only the suggested water quality standards for Fe^{3+} (0.3 ppm) in drinking water based on EPA guideline [7], but also some data reported before [10,24,46-49].

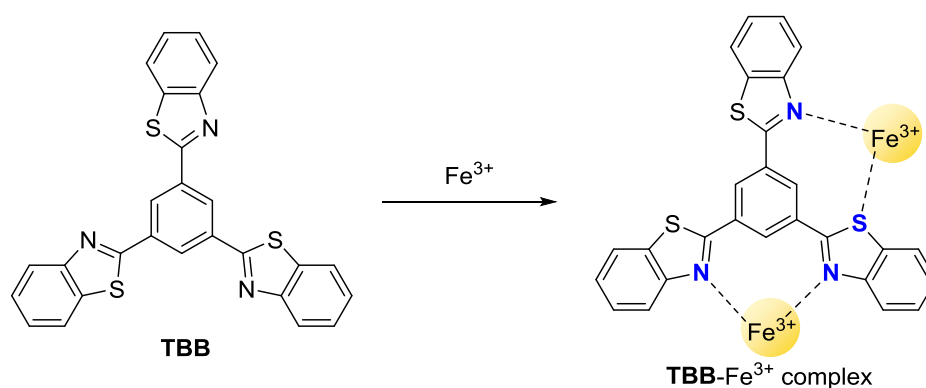
The selectivity of detecting Fe^{3+} was subsequently studied by UV-*vis* absorption and fluorescence spectra (**Fig. 4**). Each **TBB** solution with equimolar metal ion had been deposited in room temperature for three days. Delightedly, only Fe^{3+} gave rise to an apparent change in both absorption and fluorescence spectra, while the other 16 metal ions showed no obvious spectral change. This difference is probably attributed to the unique interaction between **TBB** and Fe^{3+} , which can be explained by the matching of cavity size and the radii of the guest Fe^{3+} [39]. Practically, the specific response to Fe^{3+} can also be visually distinguished in room light (**Fig. S10**). For interference study, the result is expressed through fluorescence quenching efficiency (**Fig. 5**), and it can be learnt that the quenching behaviors are almost preserved in the presence of these metal ions. Hence, **TBB** is able to selectively detect Fe^{3+} *via* optical spectra and naked-eye.

3.3. Investigation of binding mode and mechanism

The design of star-shape **TBB** was envisaged to provide two or more binding centers for coordinating with Fe^{3+} . To verify such a proposed binding behavior, the Job's plot experiment has been conducted to explore the binding stoichiometry between **TBB** and Fe^{3+} on the basis of the reported method [14]. As displayed in **Fig. 6**, the maximum fluorescence intensity emerges at a molar fraction of 0.33, indicating that the stoichiometry 1:2 is most likely binding mode for **TBB** and Fe^{3+} .

Depending on the aforementioned fluorometric titration data, the Benesi-Hildebrand plot in terms of 1:2 stoichiometry presented in good linearity (**Fig. S11**), and the Benesi-Hildebrand equation refers to: $1/(I_0 - I) = 1/\{K_a(I_0 - I_{\min})[\text{Fe}^{3+}]^2\} + 1/(I_0 - I_{\min})$, where I_0 is the initial fluorescence intensity of probe in the absence of Fe^{3+} , I_{\min} is the fluorescence intensity at saturation point. I is the fluorescence intensity measured in presence of Fe^{3+} . The calculated association constant value K_a is $1.62 \times 10^5 \text{ M}^{-2}$. This clearly implies the strong affinity between **TBB** and Fe^{3+} .

Furthermore, positive-ion ESI-MS spectrum of **TBB** with 100 equiv. $\text{Fe}(\text{NO}_3)_3$ in water/THF solution ($v/v = 4/6$) shows a peak at m/z 1011.56 (**Fig. S12**). It is assignable to $[\text{TBB} + 2\text{Fe}^{3+} + 6\text{NO}_3^- + \text{CH}_3\text{OH} + \text{H}_2\text{O} + \text{H}^+]^+$ [calcd, 1011.88]. This also evidently confirms the 1:2 ratio of the complex. Moreover, since N atom is more likely to coordinate with Fe^{3+} compared to S atom [11,37], one Fe^{3+} may bind with two N atoms on two benzothiazole moieties, while another Fe^{3+} may bind with the residual N atom and one S atom as relatively weak coordination. Based on the above analyses, the conceivable binding mode with the similar binding sites to the reported Fe^{3+} probes [11,16] is proposed in **Scheme 2**.



Scheme 2. The proposed binding mode of probe **TBB** and Fe^{3+} .

On the basis of the previous UV-*vis* absorption studies, the fluorescence quenching may involve a static process due to the formation of ground-state complexes and metal to ligand charge transfer (MLCT) reaction between **TBB** and paramagnetic Fe^{3+} [50-52]. To gain insight of the quenching mechanism, we converted the fluorometric titration results into the form of Stern-Volmer plot as shown in **Fig. 7**. It can be found that the plots show linearity at lower concentration of Fe^{3+} (0-25 μM), which stands for the involvement of static quenching through the formation of a non-fluorescent ground-state complex at lower concentration, and the quenching constant (K_{sv}) is therefore calculated to be $3.512 \times 10^3 \text{ M}^{-1}$. On the other hand, a steep curve at a higher concentration of Fe^{3+} is possibly due to dynamic quenching [53-55].

To further ascertain the quenching process, the lifetime measurement of **TBB** was then performed by time-correlated single photon counting (TCSPC) in the absence and presence of the Fe^{3+} (**Fig. S13**). The lifetime data are summarized into **Table 1**. The decay of the **TBB** solution is single-exponentially fitted, and its lifetime (τ) is 1.21 ns. Once adding Fe^{3+} of 20 and 50 equiv. respectively, τ is reduced to 1.11 ns and 0.99 ns correspondingly. These results indicate that the factor of collisional dynamic quenching exists in this process [53,55,56].

3.4. Response time

Time-response is a vital evaluation for the properties of probes [15,57]. Hence, the time dependence on the fluorescence intensity of **TBB** towards Fe^{3+} in $\text{H}_2\text{O}/\text{THF}$ ($v/v = 4/6$) was also investigated and recorded in **Fig. 8**. It can be observed that the coordination mainly happens in the first 50 seconds and finally reaches to steady state in the remained measured time. This phenomenon sufficiently demonstrates that there is a quick response of **TBB** towards Fe^{3+} , and the response time is shorter than that of some reported Fe^{3+} probes as real time detection [4,7,25,26,57] (**Table S2**).

3.5. pH effect on detection of Fe^{3+}

To explore the stability of the fluorescent detection for Fe^{3+} , we have studied the fluorescence intensity of **TBB** in $\text{H}_2\text{O}/\text{THF}$ ($v/v = 4/6$) varying different pH values from 1 to 12 (**Fig. 9**). To our delight, the fluorescence intensity of **TBB** solution exhibits ignorable variation in the wide pH range of 3-12, although there is a sharp decrease in the pH range of 1-2. Perhaps, **TBB** undergoes a protonation in strong acidic environment, leading to fluorescent change caused by charge transfer. Consequently, **TBB** possesses good tolerability in medium-strong acidic and alkaline solution. This result is superior to that of other reported Fe^{3+} probes [10,15,24,38,46], and enables **TBB**'s detection to be suitable over most of the surrounding environment.

3.6. Determination of Fe^{3+} in water samples

In order to further develop the practical application of **TBB**, a calibration curve for the determination of Fe^{3+} was constructed (**Fig. S14**), showing a good linear relationship between the fluorescence intensity of **TBB** and Fe^{3+} concentration (0-0.5 mM). Later on, drink water, tap water

and lake water were prepared as different real water samples and each of them was investigated for 5 groups of known Fe^{3+} concentration. As shown in **Table 2**, the obtained recoveries and corresponding Relative Standard Deviation (R.S.D) are satisfactory. Thus, this directly confirms the quantitative detecting ability of **TBB** toward Fe^{3+} in real water samples as the reported [58,59].

4. Conclusions

In summary, a star-shape probe based on benzothiazole moieties has been synthesized *via* simple method. It can selectively detect Fe^{3+} through fluorescence spectra over other metal ions in aqueous system ($\text{H}_2\text{O}/\text{THF}$, v/v = 4/6), and its fast response of 50 s meets the requirement for real time detection. Noteworthily, this probe possesses not only favorable stability for Fe^{3+} detection in wide pH range of 3-12, but also good performance in terms of quantitative determination for Fe^{3+} in real water samples.

Acknowledgements

We are grateful to the Guangzhou Science and Technology Project Scientific Special (General Items, No. 201607010251), Guangdong Provincial Science and Technology Project (No. 2017A010103016) and NSF of Guangdong Province (No. 2014A030313429) for financial support.

References

- [1] K. P. Carter, A. M. Young, A. E. Palmer, Fluorescent sensors for measuring metal ions in living systems, *Chem. Rev.* 114 (2014) 4564-4601.
- [2] Y. M. Ma, V. Abbate, R. C. Hider, Iron-sensitive fluorescent probes: monitoring intracellular iron pools, *Metallomics* 7 (2015) 212-222.

- [3] C. H. Fan, X. M. Huang, L. H. Han, Z. L. Lu, Z. Wang, Novel colorimetric and fluorescent off-on enantiomers with high selectivity for Fe³⁺ imaging in living cells, *Sens. Actuators, B* 224 (2016) 592-599.
- [4] X. T. Li, Y. Yin, J. J. Deng, H. X. Zhong, J. Tang, Z. Chen, L. T. Yang, L. J. Ma, A solvent-dependent fluorescent detection method for Fe³⁺ and Hg²⁺ based on a rhodamine B derivative, *Talanta* 154 (2016) 329-334.
- [5] S. K. Sahoo, D. Sharma, R. K. Bera, G. Crisponi, J. F. Callan, Iron(III) selective molecular and supramolecular fluorescent probes, *Chem. Soc. Rev.* 41 (2012) 7195-7227.
- [6] K. Vijay, C. Nandi, S. D. Samant, Synthesis of a dihydroquinoline based fluorescent cyanine for selective, naked eye, and turn off detection of Fe³⁺ ions, *RSC Adv.* 6 (2016) 49724- 49729.
- [7] B. B. Zhang, H. Y. Liu, F. X. Wu, G. F. Hao, Y. Z. Chen, C. Y. Tan, Y. Tan, Y. Y. Jiang, A dual-response quinoline-based fluorescent sensor for the detection of Copper (II) and Iron(III) ions in aqueous medium, *Sens. Actuators, B* 243 (2017) 765-774.
- [8] V. Lakshmi, M. Ravikanth, Boron-dipyrromethene based multi-anionic sensor and a specific cationic sensor for Fe³⁺, *J. Mater. Chem. C* 2 (2014) 5576-5586.
- [9] M. Saleem, S. K. Kang, K. H. Lee, Microwave assisted synthesis of a novel optical chemosensor for selective Fe³⁺ detection, *J. Lumin.* 162 (2015) 14-24.
- [10] Y. M. Liu, J. Y. Zhang, J. X. Ru, X. Yao, Y. Yang, X. H. Li, X. L. Tang, G. L. Zhang, W. S. Liu, A naked-eye visible and turn-on fluorescence probe for Fe³⁺ and its bioimaging application in living cells, *Sens. Actuators, B* 237 (2016) 501-508.
- [11] J. Geng, Y. Liu, J. H. Li, G. Yin, W. Huang, R. Y. Wang, Y. W. Quan, A ratiometric fluorescent probe for ferric ion based on a 2,2'-bithiazole derivative and its biological applications, *Sens. Actuators, B* 222 (2016) 612-617.
- [12] P. Li, M. Zhang, X. K. Sun, S. W. Guan, G. Zhang, M. Baumgarten, K. Müllen, A dendrimer-based highly sensitive and selective fluorescence quenching sensor for Fe³⁺ both in solution and as film, *Biosens. Bioelectron.* 85 (2016) 785-791.

- [13] S. K. Sahoo, D. Sharma, A. Moirangthem, A. Kuba, R. Thomas, R. Kumar, A. Kumar, H. J. Choi, A. Basu, Pyridoxal derived chemosensor for chromogenic sensing of Cu^{2+} and fluorogenic sensing of Fe^{3+} in semi-aqueous medium, *J. Lumin.*, 172 (2016) 297-303.
- [14] L. X. Lan, Q. F. Niu, Z. R. Guo, H. X. Liu, T. D. Li, Highly sensitive and fast responsive “turn-on” fluorescent sensor for selectively sensing Fe^{3+} and Hg^{2+} in aqueous media based on an oligothiophene derivative and its application in real water samples, *Sens. Actuators, B* 24 (2017) 500-508.
- [15] T. T. Xu, J. X. Yang, J. M. Song, J. S. Chen, H. L. Niu, C. J. Mao, S. Y. Zhang, Y. H. Shen, Synthesis of high fluorescence graphene quantum dots and their selective detection for Fe^{3+} in aqueous solution, *Sens. Actuators, B* 24 (2017) 863-872.
- [16] T. Sun, Q. F. Niu, Y. Li, T. D. Li, H. X. Liu, Novel oligothiophene-based dual-mode chemosensor: “Naked-Eye” colorimetric recognition of Hg^{2+} and sequential off-on fluorescence detection of Fe^{3+} and Hg^{2+} in aqueous media and its application in practical samples, *Sens. Actuators, B* 248 (2017) 24-34.
- [17] Y. Qian, J. F. Liu, A novel naphthalimide-rhodamine dye: Intramolecular fluorescence resonance energy transfer and ratiometric chemodosimeter for Hg^{2+} and Fe^{3+} , *Dyes Pigm.* 136 (2017) 782-790.
- [18] M. Kamaci, İ. Kaya, A highly selective, sensitive and stable fluorescent chemosensor based on Schiff base and poly(azomethine-urethane) for Fe^{3+} ions, *J. Ind. Eng. Chem.* 46 (2017) 234-243.
- [19] E. N. Kaya, F. Yuksel, G. A. Özpınar, M. Bulut, M. Durmuş, 7-Oxy-3-(3,4,5-trimethoxy- phenyl) coumarin substituted phthalonitrile derivatives as fluorescent sensors for detection of Fe^{3+} ions: Experimental and theoretical study, *Sens. Actuators, B* 194 (2014) 377-388.
- [20] N. R. Chereddy, P. Nagaraju, M. V. N. Raju, V. R. Krishnaswamy, P. S. Korrapati, P. R. Bangal, V. J. Rao, A novel FRET ‘off-on’ fluorescent probe for the selective detection of Fe^{3+} , Al^{3+} and Cr^{3+} ions: Its ultrafast energy transfer kinetics an application in live cell imaging, *Biosens. Bioelectron.* 68 (2015) 749-756.

- [21] B. L. Sui, S. M. Tang, T. H. Liu, B. S. Kim, K. D. Belfield, Novel BODIPY-based fluorescence turn-on sensor for Fe^{3+} and its bioimaging application in living cells, *ACS Appl. Mater. Interfaces* 6 (2014) 18408-18142.
- [22] Y. W. Choi, G. J. Park, Y. J. Na, H. Y. Jo, S. A. Lee, G. R. You, C. Kim, A single Schiff base molecule for recognizing multiple metal ions: A fluorescence sensor for Zn(II) and Al(III) and colorimetric sensor for Fe(II) and Fe(III), *Sens. Actuators, B* 194 (2014) 343-352.
- [23] S. Erdemir, O. Kocyigit, Anthracene excimer-based "turn on" fluorescent sensor for Cr^{3+} and Fe^{3+} ions: Its application to living cells, *Talanta* 158 (2016) 63-69.
- [24] R. Kagit, M. Yildirim, O. Ozay, S. Yesilot, H. Ozay, Phosphazene based multicentered naked-eye fluorescent sensor with high selectivity for Fe^{3+} ions, *Inorg. Chem.* 53 (2014) 2144-2151.
- [25] X. X. Wu, S. S. Zhang, Q. F. Niu, T. D. Li, A novel urea-derived fluorescent sensor for highly selective and sensitive detection of Fe^{3+} , *Tetrahedron Lett.* 57 (2016) 3407-3411.
- [26] F. Y. Yan, T. C. Zheng, S. S. Guo, D. C. Shi, Z. Y. Han, S. Y. S. Zhou, L. Chen, New fluorescence probe for Fe^{3+} with bis-rhodamine and its application as a molecular logic gate, *Spectrochim. Acta, Part A* 151 (2015) 881-887.
- [27] Z. Chi, X. Ran, L. L. Shi, J. Lou, Y. M. Kuang, L. J. Guo, Molecular characteristics of a fluorescent chemosensor for the recognition of ferric ion based on photoresponsive azobenzene derivative, *Spectrochim. Acta, Part A* 171 (2017) 25-30.
- [28] R. S. Keri, M. R. Patil, S. A. Patil, S. Budagumpi, A comprehensive review in current developments of benzothiazole-based molecules in medicinal chemistry, *Eur. J. Med. Chem.* 89 (2015) 207-251.
- [29] S. Sarkar, A. A Siddiqui, S. J. Saha, R. De, S. Mazumder, C. Banerjee, M. S. Idbal, S. Nag, S. Adhikari, U. Bandyopadhyay, Antimalarial activity of small-molecule benzothiazole hydrazones, *Antimicrob. Agents Chemother.* 60 (2016) 4217-4228.
- [30] L. X. Zhao, X. Y. Wang, X. D. Li, W. J. Zhang, X. H. Liu, Y. J. Zhu, H.-Q. Wang, J. F. Fang, Improving performance and reducing hysteresis in perovskite solar cells by using F8BT as electron transporting layer, *Sol. Energy Mater. Sol. Cells* 157 (2016) 79-84.

- [31] H. Ju, D. J. Chang, S. Kim, H. Ryu, E. Lee, I-H Park, J. H. Jung, M. Ikeda, Y. Habata, S. S. Lee, Cation-selective and anion-controlled fluorogenic behaviors of a benzothiazole-attached macrocycle that correlate with structural coordination modes, *Inorg. Chem.* 55 (2016) 7448-7456.
- [32] Y. Z. Jin, S. Wang, Y. J. Zhang, Highly selective fluorescent chemosensor based on benzothiazole for detection of Zn^{2+} , *Sens. Actuators, B* 225 (2016) 167-173.
- [33] V. O. Rodionov, S. I. Presolski, S. Gardinier, Y. H. Lim, M. G. Finn, Benzimidazole and related ligands for Cu-catalyzed azide-alkyne cycloaddition, *J. Am. Chem. Soc.* 129 (2007) 12696-12704.
- [34] D. M. Santana, R. García-Bueno, G. García, M. J. Piernas, J. Pérez, L. García, I. Lopez- García, Benzazolate complexes of pentacoordinate nickel(II). Synthesis, spectroscopic study and luminescent response towards metal cations, *Polyhedron* 61 (2013) 161-171.
- [35] D. Kand, P. S. Mandal, A. Datar, P. Talukdar, Iminocoumarin based fluorophores: Indispensable scaffolds for rapid, selective and sensitive detection of thiophenol, *Dyes Pigm.* 106 (2014) 25-31.
- [36] Y. J. Zhang, L. M. Guan, H. Yu, Y. H. Yan, L. B. Du, Y. Liu, M. T. Sun, D. J. Huang, S. H. Wang, Reversible fluorescent probe for selective detection and cell imaging of oxidative stress indicator bisulfite, *Anal. Chem.* 88 (2016) 4426-4431.
- [37] S. D. Liu, L. W. Zhang, X. Liu, A highly sensitive and selective fluorescent probe for Fe^{3+} based on 2-(2-hydroxyphenyl)benzothiazole, *New J Chem.* 37 (2013) 821-826.
- [38] J. B. Arockiam, S. Ayyanar, Benzothiazole, pyridine functionalized triphenylamine based fluorophore for solid state fluorescence switching, Fe^{3+} and picric acid sensing, *Sens. Actuators, B* 242 (2017) 535-544.
- [39] S. Das, K. Aich, S. Goswami, C. K. Quah, FRET-based fluorescence ratiometric and colorimetric sensor to discriminate Fe^{3+} from Fe^{2+} , *New J. Chem.* 40 (2016) 6414-6420.

- [40] Y. Gao, H. M. Liu, Q. L. Liu, W. Wang, A novel colorimetric and OFF-ON fluorescent chemosensor based on fluorescein derivative for the detection of Fe^{3+} in aqueous solution and living cells, *Tetrahedron Lett.* 57 (2016) 1852-1855.
- [41] X. Zhang, J. Y. Liu, Solvent dependent photophysical properties and near-infrared solid-state excited state intramolecular proton transfer (ESIPT) fluorescence of 2,4,6-trisubstituted thiazolylphenol, *Dyes Pigm.* 12 (2016) 80-88.
- [42] L. Y. Wang, L. L. Yang, D. R. Cao, Probes based on diketopyrrolopyrrole and anthracenone conjugates with aggregation-induced emission characteristics for pH and BSA sensing, *Sens. Actuators, B* 221 (2015) 155-166.
- [43] S. Sahana, G. Mishra, S. Sivakumar, P. K. Bharadwaj, A 2-(2'-hydroxyphenyl)benzothiazole (HBT)-quinoline conjugate: a highly specific fluorescent probe for Hg^{2+} based on ESIPT and its application in bioimaging, *Dalton Trans.* 44 (2015) 20139-20146.
- [44] V. K. Gupta, N. Mergu, L. K. Kumawat, A new multifunctional rhodamine-derived probe for colorimetric sensing of Cu(II) and Al(III) and fluorometric sensing of Fe(III) in aqueous media, *Sens. Actuators, B* 223 (2016) 101-113.
- [45] D. Sharma, A. Kuba, R. Thomas, R. Kumar, H. J. Choi, S. K. Sahoo, An aqueous friendly chemosensor derived from vitamin B6 cofactor for colorimetric sensing of Cu^{2+} and fluorescent turn-off sensing of Fe^{3+} , *Spectrochim. Acta, Part A* 153 (2016) 393-396.
- [46] S. Li, D. Zhang, X. Y. Xie, S. G. Ma, Y. Liu, Z. H. Xu, Y. F. Gao, Y. Ye, A novel solvent-dependently bifunctional NIR absorptive and fluorescent ratiometric probe for detecting $\text{Fe}^{3+}/\text{Cu}^{2+}$ and its application in bioimaging, *Sens. Actuators, B* 224 (2016) 661-667.
- [47] W. Y. Lin, L. L. Long, L. Yuan, Z. M. Cao, J. B. Feng, A novel ratiometric fluorescent Fe^{3+} sensor based on a phenanthroimidazole chromophore, *Anal. Chim. Acta* 2009, 634, 262- 266.
- [48] Y. K. Chiang, Y. R. Bhorge, R. D. Divate, Y. C. Chung, Y. P. Yen, A new schiff base chemodosimeter: selective colorimetric and fluorescent detection of Fe(III) ion, *J. Fluoresc.* 26 (2016) 1699-1708.

- [49] X. M. Chen, Q. C. Zhuo, W. S. Zou, Q. S. Qu, F. Wang, A colorimetric Fe³⁺ sensor based on an anionic poly(3,4-propylenedioxythiophene) derivative, *Sens. Actuators, B* 244 (2017) 891-896.
- [50] S. S. Razi, R. Ali, R. C. Gupta, S. K. Dwivedi, G. Sharma, B. Koch, A. Misra, Phenyl-end-capped-thiophene (P-T type) based ICT fluorescent probe (D- π -A) for detection of Hg²⁺ and Cu²⁺ ions: Live cell imaging and logic operation at molecular level, *J. Photochem. Photobiol., A* 324 (2016) 106-116.
- [51] S. Bothra, Y. Upadhyay, R. Kumar, S. K. Sahoo, Applications of vitamin B6 cofactor pyridoxal 5'-phosphate and pyridoxal 5'-phosphate crowned gold nanoparticles for optical sensing of metal ions, *Spectrochim. Acta, Part A* 174 (2017) 1-6.
- [52] A. Misra, S. Mohammad, Chromo and fluorogenic properties of some azo-phenol derivatives and recognition of Hg²⁺ ion in aqueous medium by enhanced fluorescence, *J. Phys. Chem. C* 114 (2010) 16726-16739.
- [53] Y.-C. Wu, S.-H. Luo, L. Cao, K. Jiang, L.-Y. Wang, J.-C. Xie, Z.-Y. Wang, Self-assembled structures of *N*-alkylated bisbenzimidazolyl naphthalene in aqueous media for highly sensitive detection of picric acid, *Anal. Chim. Acta* 976 (2017) 74-83.
- [54] C. Wu, J. L. Zhao, X. K. Jiang, X. L. Ni, X. Zeng, C. Redshaw, T. Yamato, Click-modified hexahomotrioxacalix[3]arenes as fluorometric and colorimetric dual-modal chemosensors for 2,4,6-trinitrophenol, *Anal. Chim. Acta* 936 (2016) 216-221.
- [55] D. C. Santra, M. K. Bera, P. K. Sukul, S. Malik, Charge-transfer-induced fluorescence quenching of anthracene derivatives and selective detection of picric acid, *Chem. - Eur. J.* 22 (2016) 2012-2019.
- [56] C. Wang, J. D. Zhou, G. X. Ran, F. Li, Z. Zhong, Q. J. Song, Q. C. Dong, Bi-functional fluorescent polymer dots: a one-step synthesis via controlled hydrothermal treatment and application as probes for the detection of temperature and Fe³⁺, *J. Mater. Chem. C* 5 (2017) 434-443.

- [57] L. R. Yan, M. P. Yang, X. Leng, M. Zhang, Y. Long, B. Q. Yang, A new dual-function fluorescent probe of Fe^{3+} for bioimaging and probe- Fe^{3+} complex for selective detection of CN^- , *Tetrahedron* 72 (2016) 4361-4367.
- [58] T. G. Jo, K. H. Bok, J. Han, M. H. Lim, C. Kim, Colorimetric detection of Fe^{3+} and Fe^{2+} and sequential fluorescent detection of Al^{3+} and pyrophosphate by an imidazole-based chemosensor in a near-perfect aqueous solution, *Dyes Pigm.* 139 (2017) 136-147.
- [59] Y. S. Kim, J. J. Lee, J. J. Lee, S. Y. Lee, T. G. Jo, C. Kim, A highly sensitive benzimidazole- based chemosensor for the colorimetric detection of Fe(II) and Fe(III) and the fluorometric detection of Zn(II) in aqueous media, *RSC Adv.* 6 (2016) 61505-61515.

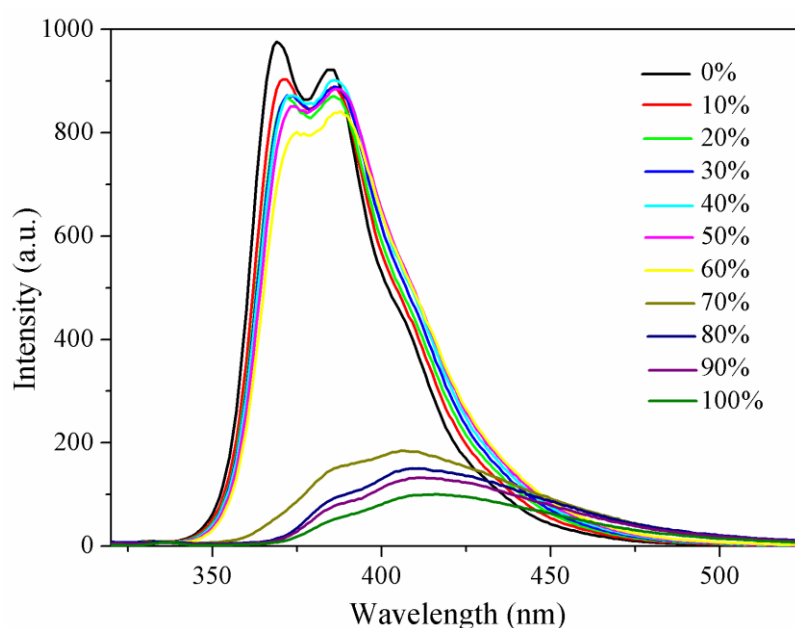


Fig. 1. The fluorescence spectra ($\lambda_{\text{ex}} = 300 \text{ nm}$) of probe **TBB** ($10 \mu\text{M}$) in $\text{H}_2\text{O}/\text{THF}$ system with different water fractions.

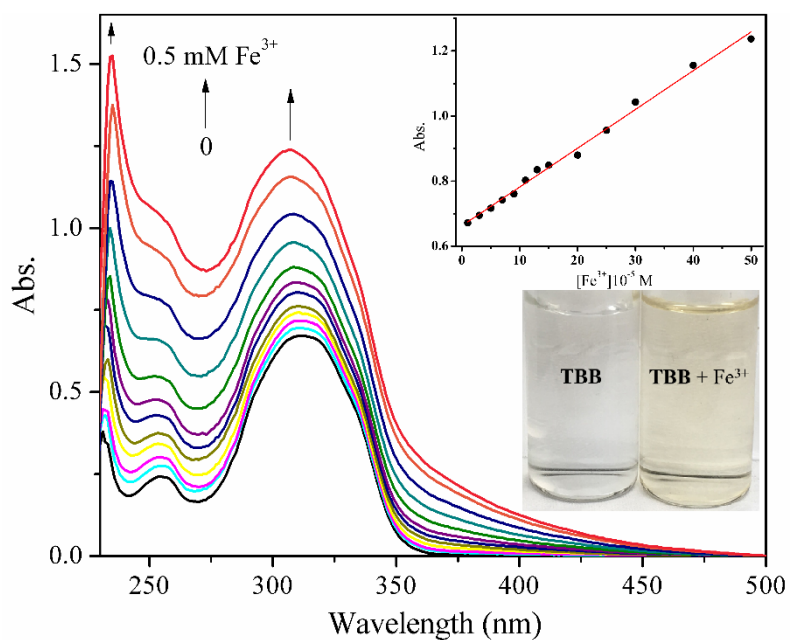


Fig. 2. UV-vis absorption spectra of **TBB** (10 μM in H₂O/THF, v/v = 4/6) with the addition of different concentrations of Fe³⁺ (0-0.5 mM). Inset, bottom right: Visual color change of **TBB** before and after addition of Fe³⁺ to 0.5 mM.

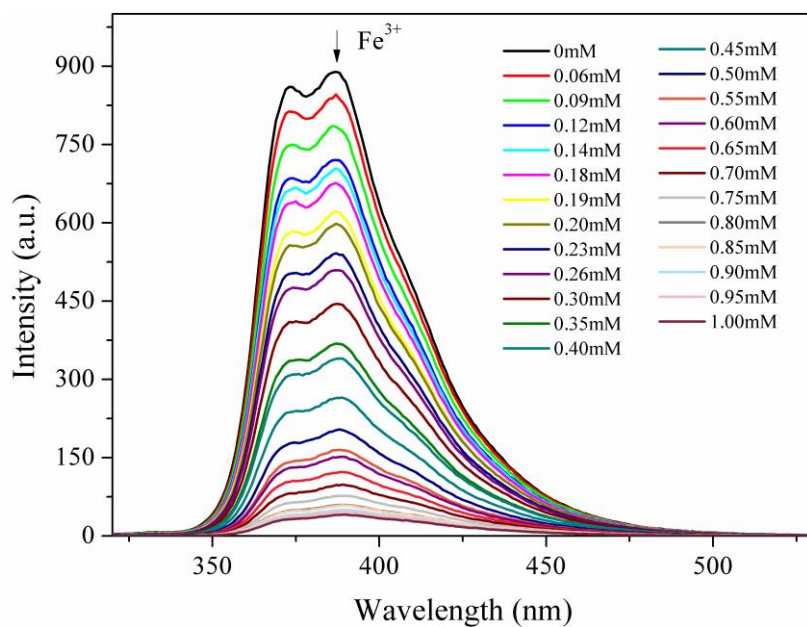


Fig. 3. The emission spectra of probe **TBB** (10 μM in H₂O/THF, v/v = 4/6) with the addition of different concentrations of Fe³⁺ (0-1 mM), λ_{ex} = 300 nm.

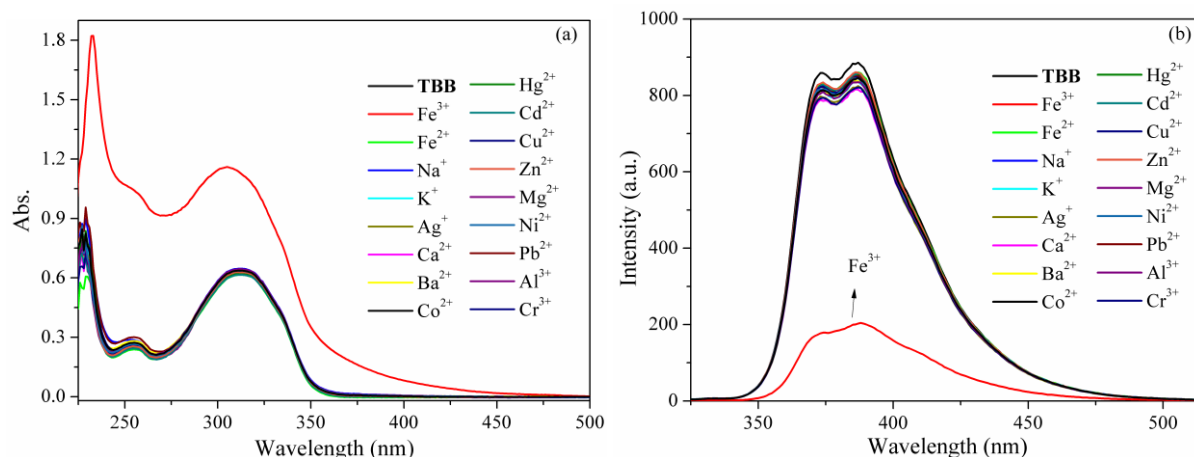


Fig. 4. Comparison of UV-vis absorption (a) and fluorescent spectra (b) of **TBB** ($10 \mu\text{M}$ in $\text{H}_2\text{O}/\text{THF}$, $v/v = 4/6$) after the addition of 0.5 mM of various metal ions.

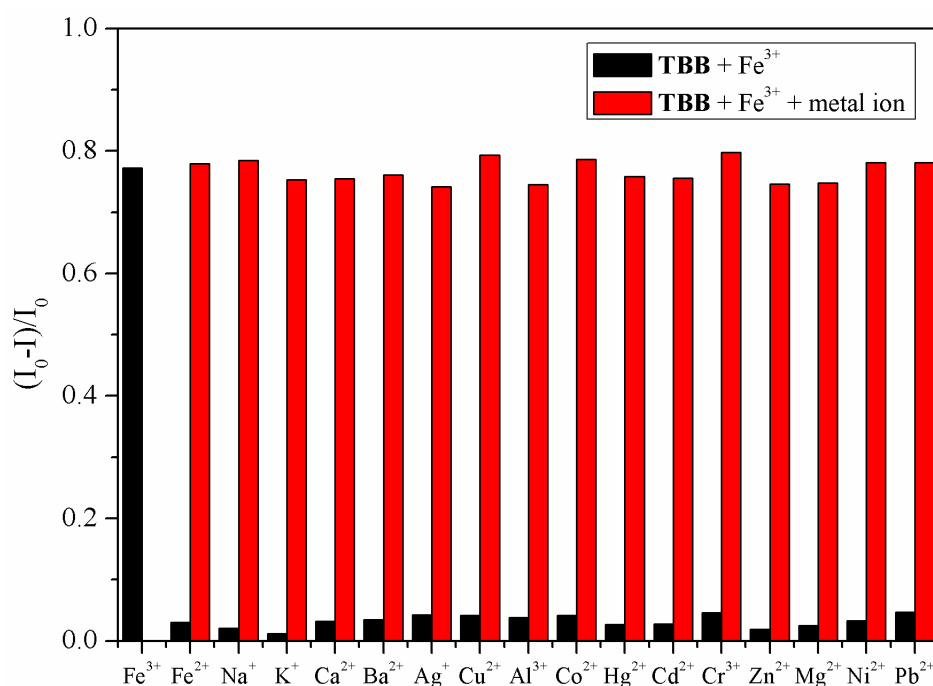


Fig. 5. Comparison of fluorescence quenching efficiency of **TBB** ($10 \mu\text{M}$ in $\text{H}_2\text{O}/\text{THF}$, $v/v = 4/6$) upon addition of different metal ions (0.5 mM), and with Fe^{3+} (0.5 mM) in the presence of various metal ions (0.5 mM).

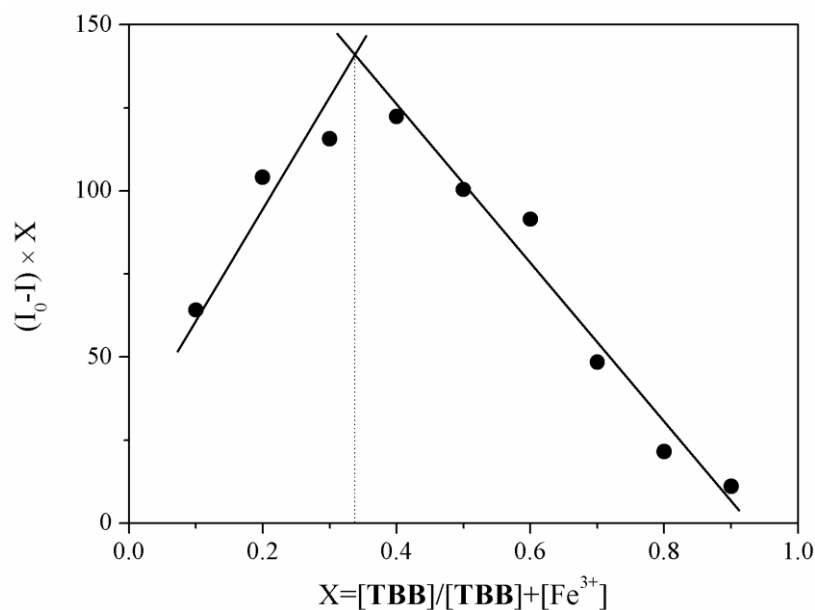


Fig. 6. Job's plot for the evolution of binding stoichiometry between **TBB** and Fe^{3+} (in $\text{H}_2\text{O}/\text{THF}$, v/v = 4/6, $\lambda_{\text{ex}} = 300 \text{ nm}$).

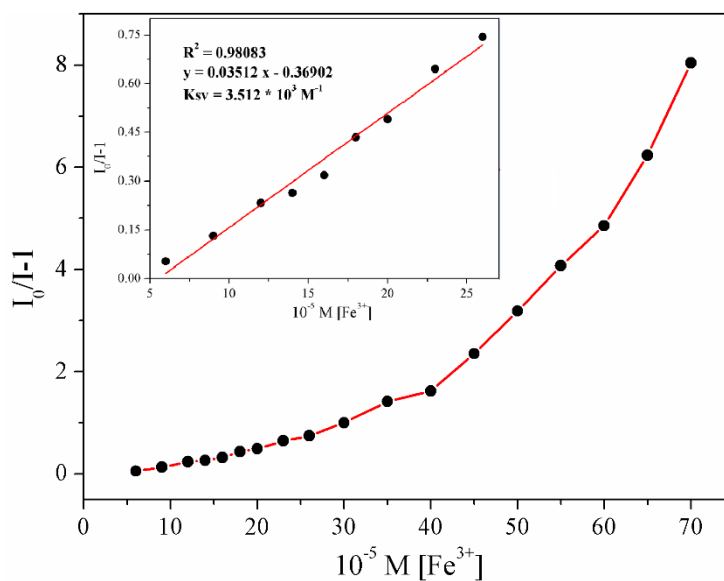


Fig. 7. Stern-Volmer plots in response to Fe^{3+} . Inset: Stern-Volmer plot obtained at lower concentration of Fe^{3+} .

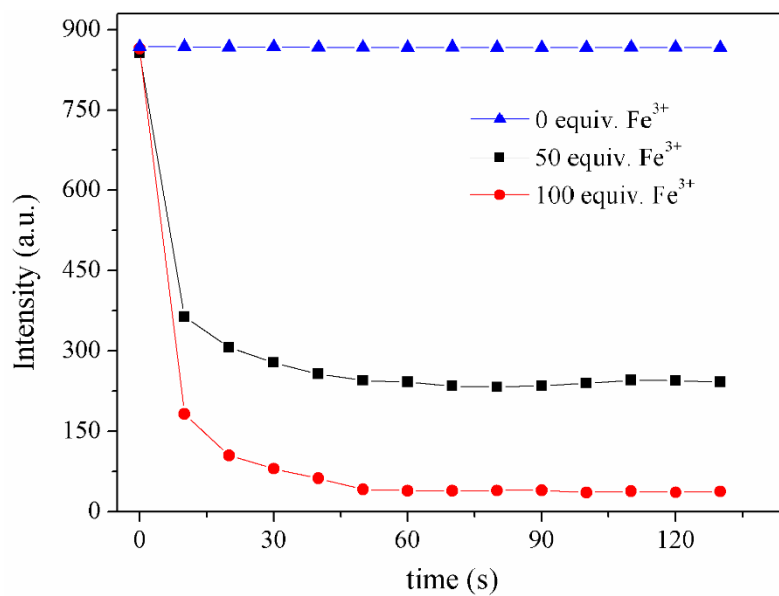


Fig. 8. Time-dependent emission intensity (at 387 nm) of probe **TBB** in H₂O/THF (v/v = 4/6).

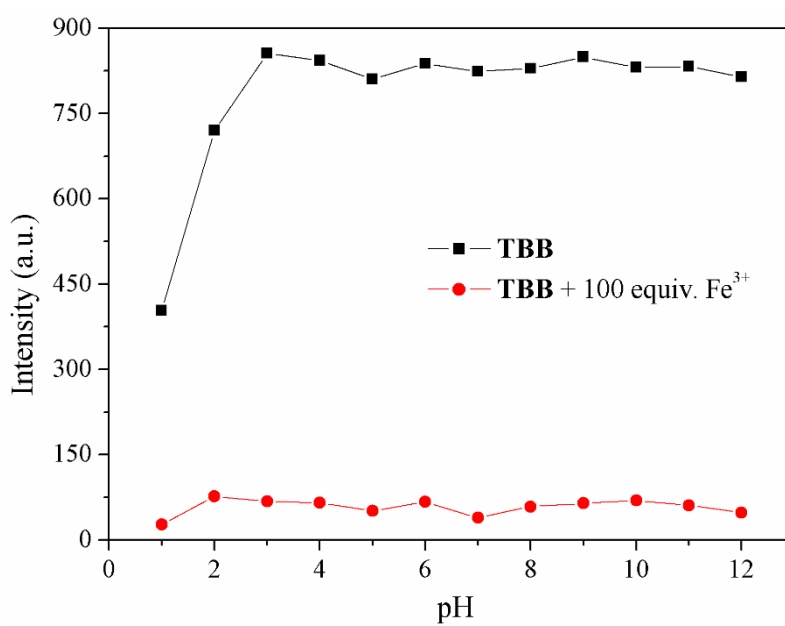


Fig. 9. Fluorescence responses at 387 nm for free **TBB** (10 μM) and after the addition of 100 equiv. Fe³⁺ in H₂O/THF (v/v = 4/6) as a function of different pH values.

Table 1 Fluorescence lifetime data for **TBB** with different equivalents of Fe^{3+} .

Sample	τ (ns)	χ^2
TBB	1.21	1.077
TBB + 20 equiv. Fe^{3+}	1.11	1.065
TBB + 50 equiv. Fe^{3+}	0.99	1.015

Table 2 Determination of Fe³⁺ in water samples.

	Fe ³⁺ added (mM)	Fe ³⁺ found (mM)	Recovery (%)	R.S.D (n=3) (%)
Drink water	0	0.0000	–	0.21
	0.1	0.0993	99.3	2.50
	0.2	0.2037	101.9	2.73
	0.3	0.3197	106.6	4.27
	0.4	0.4247	106.2	3.10
	0.5	0.4953	99.2	2.75
Tap water	0	0.0000	–	0.18
	0.1	0.0967	99.6	1.51
	0.2	0.1976	98.8	0.47
	0.3	0.3047	101.6	3.32
	0.4	0.4342	108.6	2.71
	0.5	0.5306	106.1	6.09
Lake water	0	0.0000	–	0.23
	0.1	0.0968	96.8	1.98
	0.2	0.2021	101.0	0.92
	0.3	0.3040	101.3	1.44
	0.4	0.4098	102.4	2.16
	0.5	0.5222	104.4	3.48